Nanofiltration retentate treatment from urban wastewater secondary effluent by solar electrochemical oxidation processes.

I. Salmerón[a,b], G. Rivas[a,b], I. Oller[a,b], A. Martínez-Piernas[b], A. Agüera[b], S. Malato[a,b].

[a]*Plataforma Solar de Almería-CIEMAT. Ctra Senés km 4, 04200 Tabernas (Almería), Spain.*

[b] *CIESOL, Joint Centre of the University of Almería-CIEMAT, 04120 Almería, Spain*

Abstract

Comparison of electrochemical processes at pilot plant scale for the elimination of organic microcontaminants in actual urban wastewater treatment plant secondary effluents pre-treated by nanofiltration ($[Cl^-]$ = 1100-2000 mg L^{-1}) membranes (for reducing total volume to be treated and increase water salinity), has been addressed. Anodic oxidation (AO), solar-assisted AO, electro Fenton (EF) and solar photoelectron-Fenton (SPEF) processes have been evaluated by using, when required, ethylenediamine-N,N'-disuccinic acid (EDDS) as complexing agent to maintain iron in solution at natural pH. Target water was spiked with a mix solution of microcontaminants: pentachlorophenol, terbutryn, chlorfenvinphos and diclofenac format initial concentrations of 500 and 100 μg L^{-1}, each. AO and EF processes obtained similar degradation rates as added EDDS competed with microcontaminants for oxidant species. SPEF and solar assisted AO showed that high chloride concentrations was a crucial factor since chlorine species generated by solar-assisted AO were enough for efficient microcontaminant removal avoiding the addition of EDDS. Degradation monitoring of microcontaminants contained in actual urban

wastewater treatment plant effluents was carried out by liquid chromatography coupled to hybrid quadrupole-linear ion trap-mass spectrometry. .

Keywords: Boron doped diamond, electrochemistry, micropollutants, solar-assisted electrooxidation, wastewater regeneration.

1. Introduction

The growth of chemical industry based on the development of products for personal care, pharmaceuticals or pesticides, involves the widespread in the environment of new recalcitrant substances unable to be removed by conventional secondary biological reactors in urban wastewater treatment plants. These substances are known as organic microcontaminants, which, despite being in low concentrations, in the range of ng L^{-1} - µg L^{-1}, can represent a serious concern to water bodies. Their direct impact on the ecosystem is still unknown and they can even affect humans due to their potential bioaccumulation. For this reason, the removal of microcontaminants is one of the main issues in wastewater regeneration, being crucial for the sustainability of modern chemical processes, the reuse of treated wastewater and the quality of water bodies.[1]

Separation processes have been widely applied on water regeneration. Nanofiltration or reverse osmosis commercial membranes have been applied for the removal of personal care products, drugs and pesticides from various water matrices [2] obtaining a very good quality permeate stream but also a retentate enriched with ions and microcontaminants [3-5]. Specifically, composite polyamide membranes exhibit greater rejection performance compared to other materials [2].

Electrochemical treatments can be considered highly interesting to be combined with membrane processes. They can be applied before membranes with the aim of reducing fouling [6] to prevent pore wetting enhancing the operational life of membranes [7] or after them for the treatment of the rejection streams. The main benefit when applied to

Abbreviations

AO: anodic oxidation;; BDD: boron doped diamond; COD: chemical oxygen demand; DOC: dissolved organic carbon; EDDS: Ethylenediamine-N,N'-disuccinic acid; EF: Electro-Fenton process; SPEF: Solar photoelectro-Fenton process;; ;

the retentate is the reduction on the total volume to be treated, also involving an increase of microcontaminant concentration jointly with a decrease of the electrolyte ohmic resistance (increase of salinity), and so requiring lower cell voltage which would reduce the consumption of energy [8]. Accordingly, a higher concentration of ionic species in the retentate entails a higher electrogeneration of oxidants, increasing the capacity to remove recalcitrant organic compounds [9].

Regarding electrodes material, boron doped diamond (BDD) anodes present several characteristics that make them the most suitable for wastewater depuration: i) capability of self-cleaning through fouling oxidation [10], ii) high corrosion resistance, iii) stability up to high anodic potentials, iv) high oxygen evolution over-potential, involving high reactivity towards organics oxidation and v) higher efficient use of electrical energy regarding other electrode materials [9, 11-13].

In the regeneration of high salinity wastewaters by BDD anodes, additionally to the generation of hydroxyl radicals ($^{\bullet}OH$) (E^0 = 2.8 V) at the anode surface, it is promoted the formation of a large number of oxidants in the bulk solution from dissolved ions. They are mainly active chlorine species (hypochlorous acid and hypochlorite ion, E^0 = 1.49 V, E^0 = 0.86 V, respectively) and chloride radicals (E^0 = 2.4 V) from chlorides (reactions 1-4) [14], sulphate radicals (E^0 = 2.5 - 3.1 V) (reaction 5) [15], and even ozone (E^0 = 2.07 V) as product of low-saline water electrolysis (below 20 µS cm^{-1}) (reaction 6) [16, 17], increasing the oxidative treatment capacity. The formation of oxidants in the bulk solution is limited by mass transfer as reactions are produced on the surface of the anode with limited contact area.

$$2Cl^- \rightarrow Cl_{2(aq)} + 2e^- \quad \text{(R.1)}$$

$$Cl_{2(aq)} + HO^- \rightarrow ClO^- + Cl^- + H^+ \quad \text{(R.2)}$$

$$HClO \rightleftarrows ClO^- + H^+ \quad \text{(R.3)}$$

$$Cl^- \rightarrow Cl^{\bullet} + e^- \quad \text{(R.4)}$$

$$SO_4^{2-} \rightarrow SO_4^{\bullet} + 2e^- \quad \text{(R.5)}$$

$$3H_2O \rightarrow O_3 + 6e^- + 6H^+ \quad \text{(R.6)}$$

The use of a gas diffusion electrode as cathode allows on-line H_2O_2 electrogeneration by O_2 reduction (reaction 7), so by adding iron, Fenton reactions are promoted and the process is known as electro-Fenton (EF) (reactions 8 & 9), producing an extra source of $^{\bullet}OH$ in the bulk solution [18-21]. EF together with the potentially great amount of oxidizing species that could be generated in the anode, is considered as a powerful technology for the depuration of high saline waters as it was recently demonstrated by Tawabini et al. [22].

$$O_{2(g)} + 2H^+ + 2e^- \rightarrow H_2O_2 \quad \text{(R.7)}$$

$$Fe^{2+} + H_2O_2 \rightarrow Fe^{3+} + {}^{\bullet}OH + OH^- \quad \text{(R.8)}$$

$$Fe^{3+} + H_2O_2 \rightarrow Fe^{2+} + HO_2^{\bullet} + H^+ \quad \text{(R.9)}$$

Furthermore, this process can be improved by the application of solar light, regenerating Fe^{3+} to Fe^{2+} and so allowing to occur photo-Fenton process, which is known as solar photoelectro-Fenton (SPEF) (reaction 10). SPEF also promotes the formation of chlorine radicals from the active chlorine species by radiation at 310 and 313 nm [23, 24] (reactions 11 and 12).

$$[Fe(OH)]^{2+} + h\nu \rightarrow Fe^{2+} + {}^{\bullet}OH \quad \text{(R.10)}$$

$$ClO^- + H_2O + h\nu \rightarrow Cl^{\bullet} + {}^{\bullet}OH + OH^- \quad \text{(R.11)}$$

$$HClO + h\nu \rightarrow Cl^{\bullet} + {}^{\bullet}OH \quad \text{(R.12)}$$

Working at neutral pH along EF and SPEF processes require the addition of a complexing agent to avoid iron precipitation. In this sense, EDDS is highly used as a safe and environmentally benign complexing agent in Fenton-like processes [25]. However, since Fe^{3+}:EDDS complex is photosensitive, its stability under photocatalytic processes is limited, being degraded till $Fe(OH)_3$ that immediately precipitates. A detailed study of Fe^{3+}:EDDS photodecarboxylation mechanism during solar photo-Fenton processes has been developed by Soriano-Molina et al.[26] which can be simplified in reactions 13-17[27].

$$Fe^{3+}\text{:EDDS} + h\nu \rightarrow [Fe^{3+}\text{:EDDS}]^* \quad \text{(R.13)}$$

$$[Fe^{3+}\text{:EDDS}]^* \rightarrow Fe^{2+}\text{:EDDS} + H^+ \quad \text{(R.14)}$$

$$Fe^{2+}\text{:EDDS} + H_2O_2 \rightarrow Fe^{3+}\text{:EDDS} + {}^{\bullet}OH + OH^- \quad \text{(R.15)}$$

$$Fe^{2+}\text{:EDDS} + \rightarrow Fe^{2+} + EDDS^{3-\bullet} \quad \text{(R.16)}$$

$$Fe^{2+} + H_2O_2 \rightarrow Fe(OH)_3 + {}^{\bullet}OH + OH^- \quad \text{(R.17)}$$

An exhaustive literature review has evidenced a scarce number of works focused on the evaluation of solar-assisted electrochemical processes for the depuration of real and complex wastewaters, finding only purely electrochemical processes [9, 28-30]. In consequence, it must be highlighted that one of the key strong points of the present study is the application of electrooxidation treatments not only at pilot plant scale but also to different actual wastewaters.

The present work addresses the comparison of different electrochemical treatments: anodic oxidation (AO), EF, SPEF and AO assisted by solar energy, in order to find the best alternative for the treatment of nanofiltration retentates. Two different water matrices were evaluated: a synthetic retentate with medium content of chlorides (in the

range of 550 mg L^{-1}, from natural water) and an actual wastewater with higher concentration of chlorides (in the range of 1200-2000 mg L^{-1}, after nanofiltration pre-concentration of an urban wastewater treatment plant effluent), spiked with a mix of four microcontaminants (pentachlorophenol, terbutryn, chlorphenvinfos, and diclofenac). All the processes were tested at natural pH. In the case of EF and SPEF, iron was kept in solution at natural pH by the addition of the commercial chelate Ethylenediamine-N,N'-disuccinic acid (EDDS) as iron complexing agent [31]. Once the most suitable electrochemical treatment was selected, an assay was carried out to verify the effectiveness of the process for the removal of microcontaminants actually contained in the nanofiltration retentate of an urban wastewater treatment plant effluent. Microcontaminants degradation was monitored by liquid chromatography coupled to a hybrid quadrupole/linear ion trap mass spectrometer.

2. Materials and methods

2.1 Water matrices

2.1.1 Simulated Nanofiltration Retentate

A synthetic recipe of simulated nanofiltration retentate was developed according to the composition described by Miralles-Cuevas et al. [32], of the retentate obtained from an urban wastewater treatment plant effluent from El Ejido (Almería, Spain) operating in batch mode after achieving a volume retention factor of 4. This means reducing 4 times the initial effluent volume, taking into account that nanofiltration membranes do not retain monovalent ions. Maximum values for main ions were stablished as follows: 500 mg L^{-1} of Cl^-, 1500 mg L^{-1} of SO_4^{2-}, 1050 mg L^{-1} of Na^+, 213 mg L^{-1} of Ca^{2+}, 20 mg L^{-1} of NH_4^-, 50 mg L^{-1} of Mg^{2+}, 40 mg L^{-1} of K^+ and 100 mg L^{-1} of NO_3^-. To avoid a strong

•OH scavenger effect, inorganic carbon was established at 160 mg L^{-1}, which corresponds to the natural inorganic carbon found in the tap water at the Plataforma Solar de Almería, Spain.

According to these premises, simulated nanofiltration retentate was formulated by using 82 mg L^{-1} of $Ca(NO_3)_2$ (from Sigma-Aldrich), 1420 mg L^{-1} of Na_2SO_4 (from Sigma-Aldrich), 87 mg L^{-1} of K_2SO_4 (from Merck Millipore), 340 mg L^{-1} of $CaSO_4$ (from Panreac), 497 mg L^{-1} of NaCl (from Sigma-Aldrich), 66 mg L^{-1} of $(NH_4)_2SO_4$ (from Merck Millipore) and 21 mg L^{-1} of Na_2HPO_4 (from Panreac) dissolved in natural water. The final ionic composition of the simulated nanofiltration retentate and natural water are shown in Table SI-1 (see supplementary information).

2.1.2 Urban wastewater treatment plant effluent

Actual urban wastewater treatment plant secondary effluent was collected from El Ejido (Almería, Spain) during dry season, (April - July 2019). Before experimentation, wastewater was filtered through a 75 microns sand filter and two polypropylene wound filter cartridges of 25 and 5 microns, respectively. Most significant physicochemical measured parameters were: 2.1-2.3 mS cm^{-2} of conductivity and chemical oxygen demand (COD) between 17 and 50 mg L^{-1}. The rest of the effluent characterization is shown in Table SI-2 (see supplementary information).

2.2 Chemicals

Selected target microcontaminants were pentaclorophenol, terbutryn, chlorphenvinfos and diclofenac (from Sigma-Aldrich, analytical grade). Microcontaminants were previously dissolved in methanol in two stock solutions of 2.5 and 6.25 g L^{-1} (of each microcontaminant), aiming to add to the experiments the similar amount of dissolved

organic carbon (DOC) coming from methanol, when working at low initial concentrations, between 100 – 200 µg L^{-1}, or higher, 500 µg L^{-1}.

Fe^{3+}:EDDS complex, in a concentration rate of 0.1:0.2 mM, was prepared dissolving iron (III) sulfate hydrate (~75% pure) from Panreac into acidified water (pH 2.8) in darkness conditions. After this, the desired amount of EDDS (from Sigma-Aldrich) was added stirring vigorously until the solution took a very intense yellow colour indicating the proper formation of the complex.

2.3 Analytical measurements

A LAQUAact PH110 (HORIBA) portable pHmeter was used to monitor pH. Electric conductivity was determined by a GLP 31 conductimeter from CRISON. DOC and carbonates were measured by a TOC-VCSN analyser (Shimadzu), after filtering the samples through 0.45 µm nylon filter from ASIMIO. CODwas measured by a Cell Test Spectroquant® from Merck.

Anion and cation concentrations were measured by ion chromatography in a Metrohm 850 Professional IC after sample dilution (1:10 and 1:25, *v/v*) after filtration through a 0.45 µm nylon filter from ASIMIO. For anions, it was used a Metrosep A Supp 7 150/4.0 column thermoregulated at 45˚C with 3.6 mM of sodium carbonate as eluent at 0.7 mL min^{-1}. For cations the column used was a Metrosep C6 150/4.0 with an eluent solution of 1.7 mM nitric acid and 1.7 mM dipicolinic acid at1.2 mL min^{-1}.

Free available chlorine was determined by the DPD Method 10069 from Hach, using DPD powder pillows and measuring absorbance at 530 nm. Iron concentration was measured following ISO 6332 and hydrogen peroxide following DIN 38409 H15, at 510 nm and 410 nm, respectively. The spectrophotometer used for those analyses was an Evolution 220 UV-Visible from Thermo Scientific.

Degradation of microcontaminants was monitored by a UPLC/UV Agilent Series 1200 system, equipped with a reverse phase column ZORBAX Eclipse XDB-C18 (4.6 x 50 mm, 1.8 µm particle size, Agilent Technologies). Initial conditions of the method were 90/10 (*v/v*) ultrapure water with formic acid 25 mM and acetonitrile , achieving in 14 min 100% acetonitrile at a flow rate of 1 mL min^{-1}. Inyection volume was 100µL. Sample preparation before analysis consisted on a filtration step of 9 mL of the sample through a 0.22 µm hydrofobic polytetrafluoroethylene (PTFE) membrane filter from Millipore Millex. Then, the filter was flushed with 1 mL of acetonitrile in order to extract any absorbed compound. Analytical characteristics of the microcontaminantsanalyzed by UPLC/UV are shown in Table SI-3 (see supplementary information).

Fe^{3+}:EDDS concentration was determined by a HPLC Agilent 1100 Series with a reversed-phase column Luna C18 (150 x 3.00 mm, 5µm particle size), using an isocratic method 95/5 (*v/v*) on buffer solution (2 mM tetrabutylammonium bisulfate - 15 mM sodium formiate) and methanol. Inyection volume was 20 µL with a flow rate of 0.5 mL min^{-1}. Maximun absortion of Fe^{3+}:EDDS occurs at 240 nm, and the limit of quantification was 0.005 mM.

Evaluation of microcontaminants contained in actual urban wastewater treatment plant secondary effluents was carried out by a liquid chromatography system (Agilent 1200 Series) coupled to a hybrid quadrupole-linear ion trap-mass spectrometer 5500 QTRAP® from Sciex Instruments equipped with an electrospray source (TurboIon Spray), operating in positive polarity. The analytical column was a Kinetex C18 column (150 x 4.6 mm, 2.6-µm particle size; Phenomenex) operated at a constant flow rate of 0.5 mL min^{-1} and using an injection volume of 10 µL. Eluent A was 0.1% formic acid in

ultrapure water and eluent B was pure methanol. The analytical gradient was as follows: elution started with 20% B for 0.5 min, increased to 50% B within 3 min, and to 100% within 9.5 min, kept constant for 3.5 min and reduced to 20% B in 0.1 min. The total analysis run time was 13.1 min and the post-run equilibration time 6 min. The source settings were: ion spray voltage 5000 V; curtain gas 25 (arbitrary units); GS1 50 psi; GS2 40 psi; and 500 ºC. N_2 served as nebulizer, curtain and collision gas. Compounds were analysed by multiple reaction monitoring . To increase the sensitivity of the analytical method, the Schedule MRM™ algorithm was applied with a retention time window of 40 s per transition. The optimal MS/MS parameters for each compound are summarized in Table SI-4 (see supplementary information). Sciex Analyst version 1.6.2 software was used for data acquisition and processing. MultiQuant 3.0.1 software was used for quantification purposes.

2.4 Experimental Set-up

2.4.1 Preliminary Fe^{3+}:EDDS complex stability tests

Stability of Fe^{3+}:EDDS in each tested water matrix was evaluated. Also the possible interactions with the highest positive charge ions were studied, as well as the oxidant effect of hypochlorite to Fe^{3+}:EDDS. Experiments were carried out in 1 L borosilicate stirring flasks in the dark. Water matrices used during the tests were demineralized water, demineralized water with 50 mM of Na_2SO_4 and simulated nanofiltration retentate. For checking Mg^{2+} and Ca^{2+} effect, $MgSO_4$ and $CaSO_4$ were added in the concentration required to attain the same amount of divalent cations found in the simulated nanofiltration retentate, that is 247.6 mg L^{-1} and 724.8 mg L^{-1}, respectively. Finally, hypochlorite effect was checked by adding 10 and 20 mg L^{-1} (as NaClO) in demineralized water.

2.4.2 Nanofiltration pilot plant

Nanofiltration system (Fig. 1a and b) was composed by 400 L polypropylene feeding tank, 2.2 kW centrifugal pump (DP Pumps) with a frequency modulator and spiral-wound FILMTEC NF90-2540 membranes (2.6 m^2 of active area). Tests were carried out by adding the effluent to the feeding tank and passing the water through the membrane, recycling the retentate stream to the feeding tank and discarding the permeate stream. The system was operated in batch mode in order to reduce the total volume to be treated by subsequent electrooxidation processes. The feeding tank was periodically refilled to reduce 1 m^3 of urban wastewater treatment plant secondary effluent to 250 L that is a volume retention factor of 4. As nanofiltration pilot plant is controlled by a SCADA system, pressure, flow and conductivity of permeate and retentate streams were continuously monitored online.

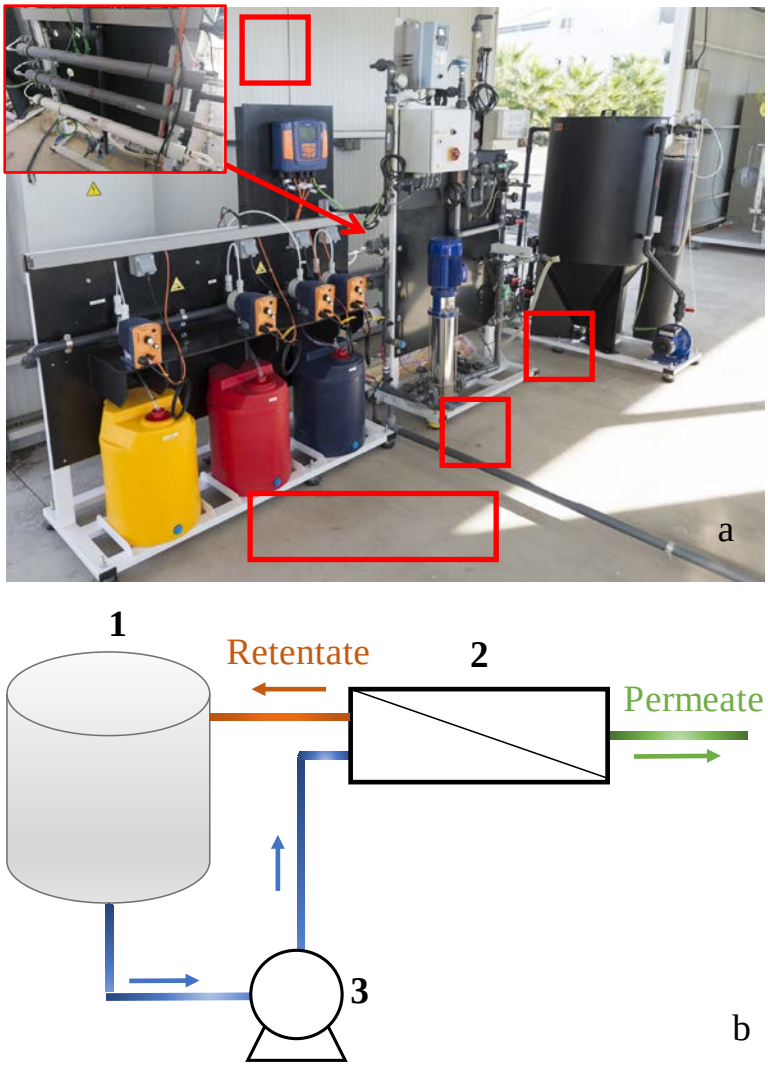

Fig. 1. a) Nanofiltration pilot plant installed at Plataforma Solar de Almería. b) Scheme of the pilot plant: 1) feeding tank, 2) nanofiltration membrane system, 3) centrifugal pump.

2.4.3 Electrooxidation pilot plant

Electrooxidation pilot plant consisted of an undivided electrochemical cell (Electro MP Cell from ElectroCell) conformed by a BDD film on a niobium mesh substrate as anode and a carbon-PTFE gas diffusion electrode as cathode, both with 0.010 m^2 geometrical area single-sides, separated by a 6 mm gap. Carbon-PTFE gas diffusion electrode cathode was fed by compressed air (ABAC air compressor, 1.5 kW) at 10 L min^{-1} and

water flow rate in the cell was 300 L h^{-1}. When H_2O_2 electrogeneration was not necessary for AO and solar-assisted AO processes, carbon-PTEF cloth was removed using the support as counter cathode. Electrodes were connected to a Delta Electronika power supply (limited to 70 V and 22 A) that fed the cell fixing a constant current density (*j*) of 74 mA cm^{-2}, optimized by Salmerón et al.[33], in order to achieve the maximum H_2O_2 electrogeneration of 64.9 mg H_2O_2 min^{-1} in the first 5 min with 50 mM of Na_2SO_4 as supporting electrolyte.

Electrochemical cell was coupled to a compound parabolic collector (CPC) photo-reactor, consisting of 10 borosilicate glass tubes mounted on an aluminium platform tilted 37º (PSA, 37º N, 2.4º W) with a total illuminated area of 2 m^2 and 23 L of illuminated volume. Working volume was 30 L in dark tests (AO and EF) and 75 L for solar-assisted electrochemical assays (solar-assisted AO and SPEF). Scheme of the solar-assisted electrooxidation pilot plant is shown in Fig. 2

Experiments were carried out by adding target wastewater (simulated nanofiltration retentate or actual retentate stream) to the reservoir of the electrooxidation pilot plant. After that, microcontaminants from the stock solution were added, recirculating till their total homogenization and verifying their initial desired concentration. At that moment AO and solar assisted AO started, but in EF and SPEF assays, Fe^{3+}:EDDS was added after microcontaminants, homogenizing before starting the process.

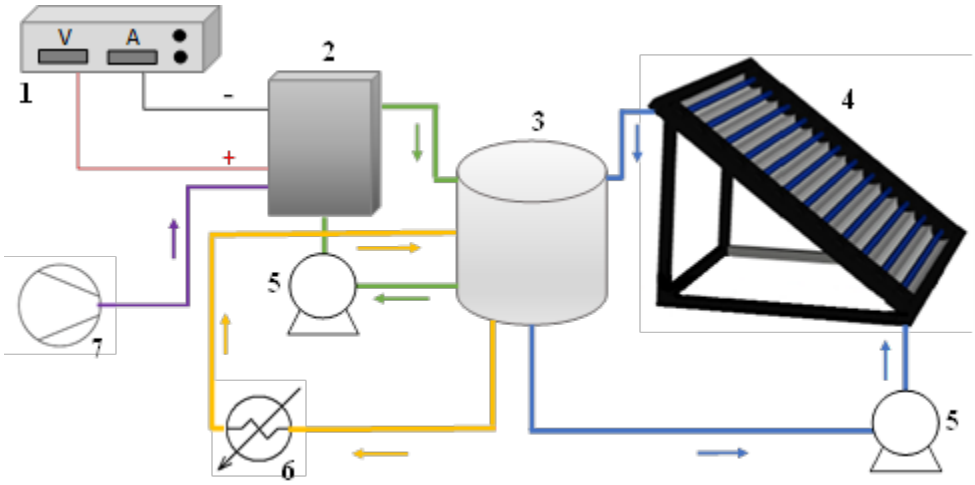

Fig. 2. Main components of the electrochemical pilot plant: 1) power supply, 2) ElectroCell with BDD anode and carbon-PTFE (gas diffusion electrode) cathode, 3) reservoir, 4) solar CPC photoreactor, 5) centrifugal pumps, 6) heat exchanger, 7) air compressor.

Temperature was always maintained between 25 and 35°C through a cooling coil connected to a heat exchanger.

Solar global ultraviolet radiation (UV) was measured with a CUV 3 UV radiometer from KIPP & ZONEN, installed at Plataforma Solar de Almería and tilted 37° same as the CPC. Equation 1 allows the combination of the data from several days of experiment and their comparison with other tests [34].

$$Q_{UV,n} = Q_{UVn-1} + \Delta t_n \cdot \overline{UV}_{G,n} \cdot A_i/V_t\,; \quad \Delta t_n = t_n - t_{n-1} \qquad \text{(Eq.1)}$$

Where $Q_{UV,n}$ (kJ L^{-1}) is the accumulated UV energy per unit of volume, $\overline{UV}_{G,n}$ (W m^{-2}) is the average solar ultraviolet radiation (λ< 400 nm) measured between t_n and t_{n-1} being n the number of sample, A_i is the irradiated surface and V_t is the total volume.

3 Results and discussion

3.1 Testing Fe^{3+}:EDDS stability

EDDS is a structural isomer of ethylenediaminetetraacetic acid but more environmentally friendly, since it is not toxic and presents high biodegradability. EDDS is completely mineralized in a short time in the environment [35], whereas other similar complexing agents are only partially degraded [36, 37]. In fact, this advantage has made EDDS one of the most studied complexing agents to keep iron in solution at neutral pH, so enhancing the production of $^{\bullet}OH$, and therefore the degradation of microcontaminants [38].

As determined by Klamerth et al. 2012 [39], Fe^{3+}:EDDS molar ratio of 1:2 is the optimal in terms of degradation and energy consumption. This ratio was successfully used by Miralles-Cuevas et al. 2014 [40] in a complex water matrix (real nanofiltration retentate with a volume retention factor of 4), for the degradation of a mix of microcontaminants in a concentration range of 47-63 μg L^{-1}, each and achieving 95% removal of the sum of microcontaminants in 86 min with a requirement of accumulated UV energy of 21.1 kJ L^{-1}.Fe^{3+}:EDDS behaviour during EF treatment by using 50 mM Na_2SO_4 solution as supporting electrolyte has been described elsewhere [41]. Nevertheless, to check the suitability of Fe^{3+}:EDDS for different electrochemical processes in a highly complex water, an EF assay was carried out with simulated nanofiltration retentate as water matrix at natural pH. Fe^{3+}:EDDS was completely degraded in 15 min despite iron continued in solution for 30 min (Fig. 3), which can be explained by the presence of oxidized species of Fe:EDDS [42].

To evaluate the possible interaction with the highest positive charge ions contained in simulated nanofiltration retentate, the stability of Fe^{3+}:EDDS was tested in the dark by

using simulated nanofiltration retentate and demineralized water containing Na_2SO_4 (50mM), $MgSO_4$ (247.6 mg L^{-1}) and $CaSO_4$ (724.8 mg L^{-1}). Fig. 3 shows, as expected, that the concentration of the complex remained constant in all cases.

As hypochlorite was going to be generated during electrochemical processes (taking into account the characterization of simulated nanofiltration retentate, as well as urban wastewater treatment plant secondary effluent, it was necessary to determine Fe^{3+}:EDDS degradation caused by this oxidant, demonstrating that with 10 and 20 mg L^{-1} of hypochlorite, Fe^{3+}:EDDS kept stable during at least one hour (data not shown).

After these preliminary tests, it was also determined that the use of this complex in electrochemical processes would be suitable for microcontaminant degradation with higher degradation rates. However, it must be stressed that, for the most recalcitrant compounds, the complex would have to be added continuously as it was degraded in 15 min, which would not be pertinent as a continuous addition of organic matter would scavenge microcontaminant degradation.

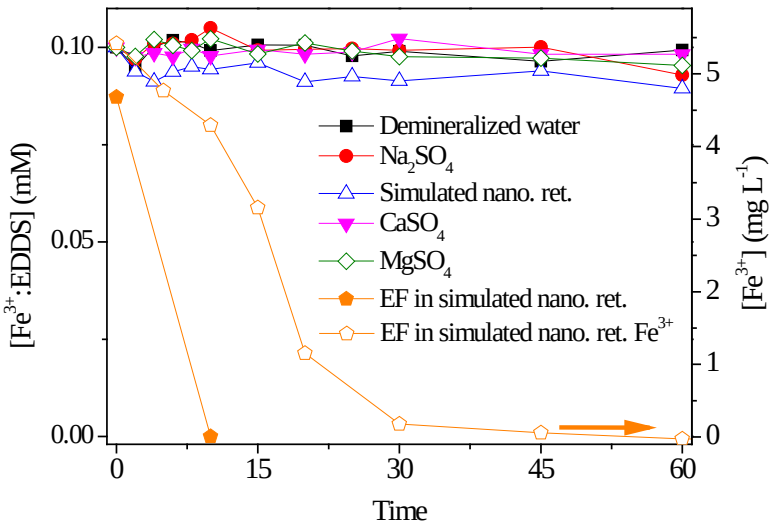

335

336 **Fig. 3.** Evolution of Fe^{3+}:EDDS in different water matrices and during EF processes in
337 simulated nanofiltration retentate matrix. Evolution of dissolved iron (Fe^{3+}) during EF
338 treatment is also plotted (against right Y axis, marked with an arrow).

339 *3.2 Electrochemical oxidation of microcontaminants contained in simulated*
340 *nanofiltration retentate*

341 As a first approach, AO, EF and SPEF, were tested for the degradation of 200 µg L^{-1} of
342 each selected microcontaminant (pentachlorophenol, terbutryn, chlorphenvinfos and
343 diclofenac) in simulated nanofiltration retentate (Fig. 4a). AO assays were developed as
344 reference, achieving the removal of 83% of the total amount of microcontaminants by
345 applying 13.9 kWh m^{-3}. The organic content, coming from the methanol of the
346 microcontaminant stock solution simulating the organic carbon of a real urban
347 wastewater treatment plant effluent (around 24 mg L^{-1}), was slightly mineralised (15%
348 of DOC removal). In the case of EF treatment, 88% of the sum of microcontaminants
349 was degraded with slightly higher energy consumption (15.6 kWh m^{-3}), showing similar
350 trend as AO. The addition of Fe^{3+}:EDDS in the EF treatment implied a theoretical
351 increase of 24 mg L^{-1} of the organic carbon (52 mg L^{-1} of total initial DOC). So, despite

the increasing in •OH production, oxidant species were mainly consumed in the mineralization process of EDDS rather than in microcontaminant degradation, which was demonstrated by the increase in the mineralization percentage till 31%. Similar results were obtained by Huang et al. 2012 [38], in which 2,2-bis-(4-hydroxyphenyl)propane degradation by photo-Fenton was inhibited when the concentration of the complex increased from 0.2 to 0.4 mM, evidencing the role of EDDS as a competitor of microcontaminants for •OH.

Moreover, in EF treatment, only 2.91 mg L^{-1} of iron remained dissolved after 15 min, being totally precipitated after 30 min. From the moment there was no iron in solution, the degradation process proceeded only through the anode action (mainly physisorbed •OH and active chlorine species)

Since EF treatment did not achieve a substantial improvement in the degradation of microcontaminants compared with AO but entailed the addition of reagents that would imply an increase in operating costs, it was discarded as an alternative for the nanofiltration retentate treatment.

In SPEF process (EF combined with a CPC photoreactor), the volume of water to be treated was much higher (75 L) than in AO or EF (30 L), while electrodes surface remained constant. The production of oxidizing species was determined by the electroactive surface area and the current applied, being the same in both configurations. However, the relative concentration of oxidants depends on the electrode area/volume ratio so lower concentrations in SPEF were reached due to the higher working volume. For such reason, despite the initial concentration of microcontaminants was the same, in terms of mass the amount was much higher in SPEF than in AO or EF.

375 In SPEF, Fe^{3+}:EDDS was also required for maintaining iron in solution at neutral pH.
376 Despite the increase in the mass of microcontaminants, it was shown an improvement in
377 the degradation rate mostly at the beginning of the treatment, due to the oxidation of
378 Fe^{2+} to Fe^{3+} that allowed photo-Fenton process occurred. Dissolved iron (5.5 mg L^{-1})
379 remained till 15 min of treatment, showing slow precipitation till 75 min, thus the
380 degradation process went on for the generation of oxidizing species in the anode and for
381 the solar promoted species. 14 kJ L^{-1} of accumulated UV energy were required for 88%
382 elimination of the sum of microcontaminants.

383 Along SPEF process the generation of H_2O_2 (Reaction 7) never exceeded an
384 accumulated value of 2.3 mg L^{-1}, which supposed an important limitation in the process.
385 In consequence, an additional SPEF test was carried out by adding 10 mg L^{-1} of H_2O_2
386 extra at the beginning of the test. In such a case, microcontaminant degradation rate
387 increased greatly, verifying the limitation provoked by the lower ratio between electrode
388 surface and total volume in SPEF compared to AO. Dissolved iron was totally
389 precipitated after 30 min but at that time 80% of microcontaminant removal was
390 achieved. At the end of the treatment 96% of microcontaminants were eliminated with
391 lower electrical energy consumption (5.9 kWh m^{-3}) and an accumulated solar UV
392 energy of 8.8 kJ L^{-1}.

393 Considering the fast removal obtained when the initial concentration of each
394 microcontaminant was 200 µg L^{-1}, it was decided to increase it to 500 µg L^{-1} for a better
395 monitoring of the operating parameters (Fig. 4b). In this case, AO achieved 70% of
396 microcontaminant removal in 30 min consuming 2.3 kWh m^{-3} of energy (28 mg L^{-1} of
397 free available chlorine and 11 mg L^{-1} of chlorates). From that point, degradation rate
398 decreased and 82% of microcontaminant degradation was attained after consuming 15
399 kWh m^{-3} accompanied by an increase of free available chlorine till 71 mg L^{-1} and

chlorates till 55 mg L^{-1}. When SPEF was applied, the removal rate increased significantly, attaining 85% microcontaminant removal with the requirement of 5.9 kWh m^{-3} of electric consumption and 10.5 kJ L^{-1} of Q_{UV} after 180 min of treatment. In this experiment, iron showed the same trend as in previous SPEF test (without adding extra amount of H_2O_2), remaining after 15 min in solution at a concentration of 4.8 mg L^{-1} and precipitating completely after 60 min. At that moment, the treatment went ahead by the action of other oxidant species (active chlorine species among them considering simulated nanofiltration retentate characterization) generated by the anode and assisted by solar energy, keeping free available chlorine stable between 22 and 31 mg L^{-1} until 120 min (chlorates concentration was 17 mg L^{-1}), when 80% of microcontaminant removal was reached.

From this point, free available chlorine started to increase till 71 mg L^{-1} at 180 min achieving 26 mg L^{-1} of chlorates. This means that the degradation promoted by active chlorine species stopped at 120 min and from that point instead of reacting with organics; they were accumulated in the solution as free available chlorine.

In view of the results obtained by SPEF, the excess of free available chlorine produced and how inefficiently it was used at the end of the treatment, it was considered to test solar-assisted AO (without the addition of iron nor the in-situ generation of H_2O_2) in order to evaluate the effect of solar energy on the electrogenerated species and the oxidants produced avoiding the addition of EDDS which competes with microcontaminants for $^{\bullet}OH$.

In solar-assisted AO, chlorides concentration (550-565 mg L^{-1} in simulated nanofiltration retentate) has a crucial role as precursors of active chlorine species. 76% of microcontaminants were degraded after an energy consumption of 5.9 kWh m^{-3} and

424 an accumulated UV energy of Q_{UV} of 11.6 kJ L^{-1}. Free available chlorine showed
425 similar behaviour as in SPEF, being constant (17 – 26 mg L^{-1}) till 150 min and
426 increasing till 85 mg L^{-1} after 180 min of treatment. As well as free available chlorine,
427 chlorates also showed same trend: 22 mg L^{-1} at 150 min and 26 mg L^{-1} at 180 min.
428 Therefore, generated active chlorine species and $Cl^{\bullet}$ in this specific wastewater were not
429 enough to completely degrade the sum of microcontaminants, evidencing the crucial
430 role of $^{\bullet}OH$ in SPEF.

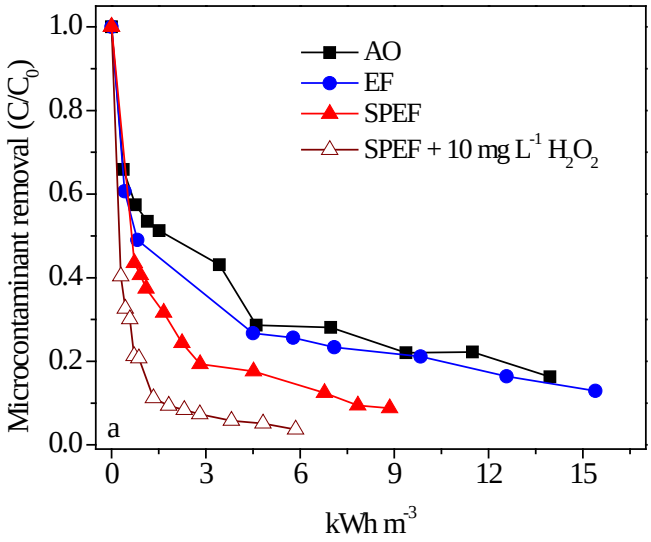

431

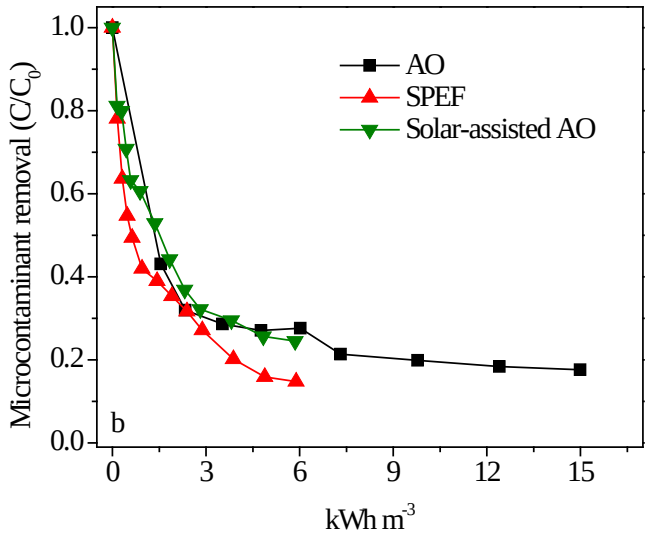

432

433 **Fig. 4.** Removal of the sum of microcontaminants (pentachlorophenol, terbutryn,
434 chlorphenvinfos and diclofenac) in simulated nanofiltration retentate by using different
435 electroxidation processes. a) initial concentration of 200 μg L^{-1} each microcontaminant b) initial
436 concentration of 500 μg L^{-1}, each microcontaminant.

437 *3.3 Actual Nanofiltration Retentate treatment by electrochemical oxidation processes*

438 Several batches (1 m^3 each) of secondary effluent were taken from the urban wastewater
439 treatment plant of El Ejido (Almería) and introduced in the nanofiltration system (till
440 attaining a volume retention factor of 4). Permeate stream generated contained only
441 some monovalent ions that passed across the membrane (DOC below 2 mg L^{-1} and
442 carbonates below 25 mg L^{-1}), thus the conductivity kept under 100 μS cm^{-1} during the
443 most of the nanofiltration process and below 200 μS cm^{-1} at the end due to the operation
444 in batch mode. In such operation mode, retentate stream was recirculated into the
445 feeding tank to reduce the total volume of final retentate and increase its conductivity
446 for obtaining a better efficiency of electrochemical processes. Table 1 shows its main
447 physicochemical characteristics.

448

449 **Table 1.** Characterization of the retentate obtained in the nanofiltration pilot plant from
450 urban wastewater treatment plant secondary effluent.

Parameter	Value	**Parameter**	Value
Conductivity (mS cm^{-1})	6.1 - 6.8	**SO_4^- (mg L^{-1})**	386 - 660
NTU	9 – 45	**Na^+ (mg L^{-1})**	747 - 787
pH	8 - 8.6	**Ca^{2+} (mg L^{-1})**	259 - 273
DOC (mg L^{-1})	31 – 42	**NH_4^+ (mg L^{-1})**	46 - 76
COD (mg L^{-1})	103 – 190	**Mg^{2+} (mg L^{-1})**	197 - 209
HCO_3^- (mg L^{-1})	1010 – 1316	**K^+ (mg L^{-1})**	62 - 71
Cl^- (mg L^{-1})	1182 – 1960	**NO_3^- (mg L^{-1})**	25 - 27

451

Commonly, actual concentration of microcontaminants in urban wastewater treatment plant effluents is very low reaching, at most, tens of μg L^{-1} as found in Luo et al. 2014 [43]. For this reason, in actual nanofiltration retentate experiments, the spiked concentration of microcontaminants was 100 μg L^{-1} each (pentachlorophenol, terbutryn, chlorphenvinfos and diclofenac), trying to address a more realistic approach jointly with a direct analysis by UPLC/UV.

From the physicochemical characterization, it must be highlighted the presence of a high concentration of carbonates in the nanofiltration retentate, which are well known scavengers of hydroxyl radicals in Fenton and photo-Fenton processes [44]. Nevertheless, their influence in electro-oxidative processes has not been defined, yet. In order to investigate this matter, each electrochemical treatment was carried out with the natural hydrogen carbonate present in the retentate stream (> 1000 mg L^{-1}), but also lowering it till 20 mg L^{-1} by adding acid and purging with air.

Results from AO (Fig. 5) showed exactly the same trend of microcontaminant degradation in high and low hydrogen carbonate concentration, achieving 84% and 83%, respectively. About DOC elimination, it was attained 9% and 12% in the presence of high and low concentration of hydrogen carbonate, respectively, remaining at the end of the treatment 17 mg L^{-1} and 4 mg L^{-1} of free available chlorine, and 47 and 42 mg L^{-1} of chlorates. In both cases results are similar, and the slight difference found can be explained due to the recalcitrant character of the organic matter contained in the different water batches used, that despite achieved higher concentration of oxidizing species, they were not able to degrade the organic content. Therefore, in our study carbonates had no substantial effect on AO or any scavenger effect on active chlorine species and $Cl^{\bullet}$.

476 This is consistent with what Xiong et al., [45] described in their study of propranolol
477 degradation with UV-LED/chlorine system testing hydrogen carbonate concentrations
478 till 840 mg L^{-1} (10 mM) without finding a remarkable difference in removal rates.

479 Regarding SPEF, retentate with high concentration of hydrogen carbonate showed 69%
480 of microcontaminant degradation applying 5.1 kWh $m^{-3}$and requiring 14.2 kJ L^{-1} of
481 accumulated UV energy. At lower concentration of hydrogen carbonate, with the same
482 electrical consumption (5.2 kWh m^{-3}) and even lower Q_{UV} (10.8 kJ L^{-1}), higher
483 microcontaminant removal was reached (75%) and thus it can be said that carbonates
484 had a slight effect on SPEF. DOC degradation was 17% in both cases, and final free
485 available chlorine was extremely low, 1.1 mg L^{-1} and 0.7 mg L^{-1} under both operating
486 conditions, which means that most of the oxidant species were consumed by the organic
487 load. Regarding chlorates, concentration reached 24 mg L^{-1} and 16 mg L^{-1} for both high
488 and low hydrogen carbonates content, respectively, showing a possible quencher effect
489 in chlorates due to the presence of carbonates in the solution.

490 Inasmuch AO process was not affected by carbonates concentration, a solar-assisted AO
491 test was developed with the retentate at natural (high) hydrogen carbonate
492 concentration. With 5.3 kWh m^{-3} and 13.8 kJ L^{-1} of accumulated UV energy, 84% of
493 microcontaminant removal was achieved, higher than in all previous experiments. Free
494 available chlorine reached was 3.9 mg L^{-1} slightly higher than in SPEF with the same
495 water matrix even with a lower DOC removal of 9%. Probably provoked by the higher
496 recalcitrant character of organic matter contained in the actual water matrix used in AO
497 and solar-assisted AO in regard with the easy mineralization of EDDS used in SPEF.
498 Chlorates measured at the end of the process were 30 mg L^{-1}, in the same range of
499 previous solar-assisted treatments (solar-assisted AO and SPEF).

In electrochemical treatments, chloride is the precursor of active chlorine species and $Cl^{\bullet}$, thus higher concentration of chloride pose higher electro-generation of active chlorine species. As described by Shu et al. [24], higher concentration of active chlorine species increased in solar processes and resulted in higher radicals generation (reactions 11 and 12), enhancing microcontaminant degradation rates. Consequently, actual nanofiltration retentate with high concentration of chloride (See table 1), showed electro-generation of higher amount of oxidants, enough to degrade the microcontaminants, avoiding the addition of any reagent and therefore, simplifying the process. In consequence, solar-assisted AO was selected as the best alternative for the treatment of nanofiltration retentates.

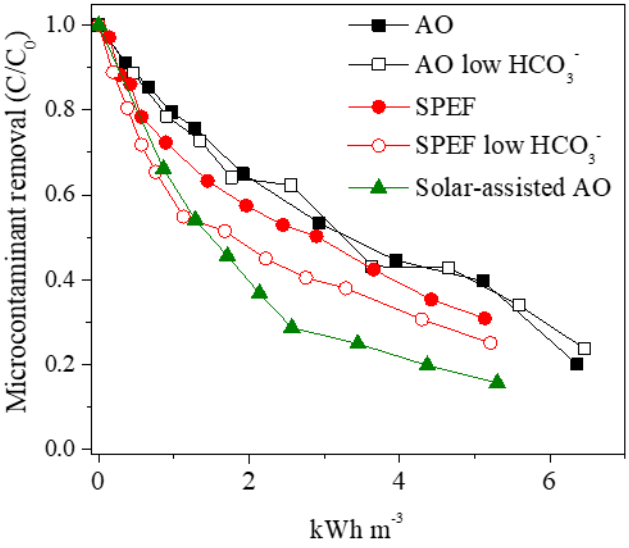

Fig. 5. Removal of the sum of microcontaminants (pentachlorophenol, terbutryn, chlorphenvinfos and diclofenac each one spiked at 100 µg L^{-1}) in actual nanofiltration retentate.

Finally, the effectiveness of solar-assisted AO was tested under complete actual conditions. A new batch of the secondary effluent of the urban wastewater treatment plant was introduced into the nanofiltration system, collecting the retentate stream (volume retention factor of 4) without reducing hydrogen carbonate concentration. Actual degradation of the microcontaminants contained in the retentate was monitored by using liquid chromatography coupled to a hybrid quadrupole-linear ion trap-mass spectrometry. A summary of the results is shown in Table 2. Detailed degradation of all microcontaminants contained in the actual effluent during electrochemical treatment, as well as their removal percentages, is shown in Table SI-5 (see supplementary information).

Table 2. Evolution of most relevant microcontaminants (> 250 ng L^{-1}) detected by liquid chromatography coupled to a hybrid quadrupole-linear ion trap-mass spectrometry.in the urban wastewater treatment plant secondary effluent, as well as their final removal percentage, nanofiltration retentate and their concentration after solar-assisted AO.

	Microcontaminants	El Ejido secondary effluent (ng L^{-1})	Nanofiltration Retentate (ng L^{-1})	After solar-assisted AO (ng L^{-1})	Removal (%) in solar-assisted AO
1	4FAA	7440	28360	780	97
2	4AAA	3660	14350	360	98
3	Gabapentin	3250	12385	2730	78
4	Carbamazepine	1945	7070	3940	44
5	Iminostilbene	1500	5775	3410	41
6	4AA	1170	4580	ND	>99
7	Imidacloprid	1200	4525	2090	54
8	Sulpiride	1045	4060	13	>99
9	Venlafaxine	750	2930	ND	>99
10	Levofloxacin	490	1930	ND	>99
11	Cetirizine	435	1690	1030	39
12	Telmisartan	420	1590	1275	20
13	Irbesartan	400	1550	905	42
14	Diatrizoic acid	380	1460	690	53

15	OMCs < 250 ng L^{-1}	1960	7500	1730	77

*ND: Non detected

Up to forty-four microcontaminants were detected in the secondary effluent of the urban wastewater treatment plant, highlighting the presence of 4FAA, 4AAA, (dipyrone metabolites) and gabapentin (antiepileptic) which were found in the highest concentrations, 7440, 3660 and 3250 ng L^{-1}, respectively. Eleven microcontaminants were detected at relevant concentrations between 300 and 2000 ng L^{-1} as carbamazepine, iminostilbene and others (see Table 2). The rest of microcontaminants were detected at lower concentrations (< 250 ng L^{-1}), being mainly pharmaceuticals as naproxen, diazepam, propanolol or flecainide.

After nanofiltration pre-treatment, 99040 ng L^{-1} of total microcontaminants were found in the retentate stream. After 90 min of solar-assisted AO application to the retentate, with 2.7 kWh m^{-3} of electric consumption and a Q_{UV} of 4.2 kJ L^{-1}, fourteen microcontaminants were substantially degraded (>99%): 4AA, lincomicin, fenofibric acid, indomethacin, naproxen, propranolol, dimethoate, erythromycin, metronidazole, sulfathiazole, trimethoprim, levofloxacin, alfuzosin, domperidone, propafenone, memantine and trazodone. At that point, DOC removal was 9% and measured free available chlorine was only 2.6 mg L^{-1}, indicating the high oxidative power of the process.

At the end of the treatment, 80% of the total amount of microcontaminants detected in the nanofiltration retentate was eliminated (Fig. 6). Energy consumption at the end of the treatment was 5.5 kWh m^{-3} and the required accumulated UV energy was 11.5 kJ L^{-1}. Final DOC removal was similar to previous cases, 19%, and free available chlorine was 8.8 mg L^{-1}. This increase in free available chlorine, from 2.6 to 8.8 mg L^{-1} at the end of the process, means that active chlorine species was not able to efficiently react

555 with the organic compounds still remaining in nanofiltration retentate, much more
556 recalcitrant to oxidation than initial organics, after suffering several oxidation steps (but
557 not mineralized). As it was observed in previous tests, chlorates are generated
558 continuously regardless microcontaminant removal, so the kinetic constant of chlorates
559 generation was calculated: 1.47 ± 0.02 (10^{-1} min^{-1}) (R^2 = 0.996).

560 Despite being among the pollutants with an important presence (> 250 ng L^{-1}), it is
561 remarkable the low removal of telmisartan (20%). Same applies to other compounds
562 such as carbamazepine or iminostilbene, two tricyclic compounds that, despite being
563 detected at higher concentrations than other microcontaminants (> 1.5 µg L^{-1}), showed
564 higher stability being only able to reach degradation rates lower that 50%.

565

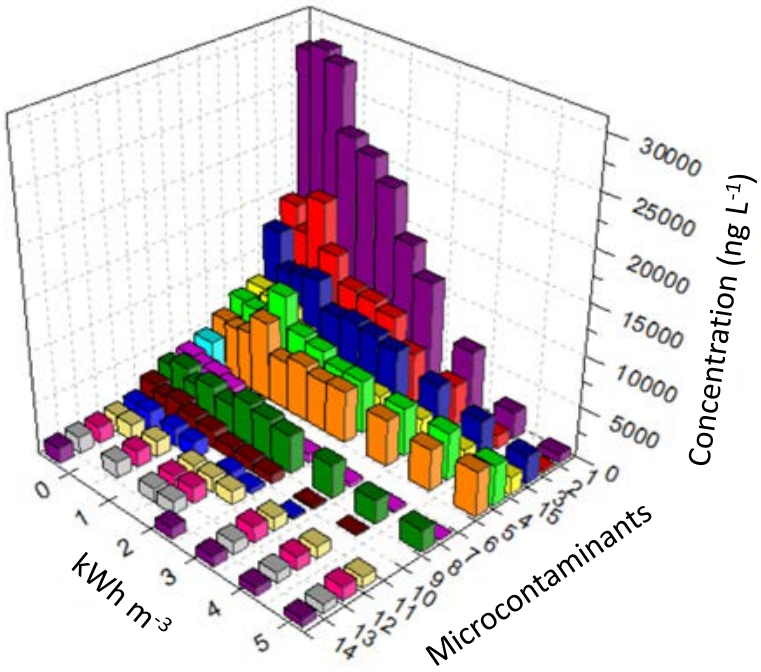

566

567 **Fig. 6.** Removal of microcontaminants contained in actual nanofiltration retentate from
568 secondary effluent of an urban wastewater treatment plant along solar-assisted AO
569 treatment.

Conclusions

It has been demonstrated that the combination of an electrochemical device with a solar CPC reactor entails an enhancement in microcontaminant removal percentages regarding pure electrooxidative processes, due to the generation of higher amount of oxidative species.

EDDS has been a useful tool to keep iron in solution in solar-assisted processes but taking into consideration that it is only effective during the first part of the treatment due to its degradation by the electrochemical process itself.

If the effluent contains a high concentration of chloride, the use of Fe^{3+}:EDDS could be avoided as only with solar-assisted AO, enough oxidant species can be generated for the complete degradation of microcontaminants.

Combined process, nanofiltration and solar-assisted electrooxidation, was successfully applied for the removal of microcontaminants of an actual urban wastewater treatment plant secondary effluent, reaching high degradation for most of them and 80% of elimination of the total amount. On the contrary, it is important to stress that this process is not effective for DOC removal. Such good performance on high elimination percentage of microcontaminants led to the possibility of obtaining high quality treated water (for instance, for reusing purposes), bearing witness on high sustainability of evaluated technologies.

Finally it important to mention that the measurement of high concentrations of chlorates at the end of the electrochemical treatments, makes necessary the performance of risk and health assessment studies before considering the reuse of treated wastewater for crops irrigation.

Acknowledgements

The authors wish to thank the Spanish Ministry of Science, Innovation and Universities (MCIU), AEI and FEDER for funding under the CalypSol Project (Reference: RTI2018-097997-B-C32).

References

[1] M. Patel, R. Kumar, K. Kishor, T. Mlsna, C.U. Pittman, Jr., D. Mohan, Pharmaceuticals of Emerging Concern in Aquatic Systems: Chemistry, Occurrence, Effects, and Removal Methods, Chem. Rev., 119 (2019) 3510-3673.

[2] K.V. Plakas, A.J. Karabelas, Removal of pesticides from water by NF and RO membranes — A review, Desalination, 287 (2012) 255-265.

[3] C. Fonseca Couto, L.C. Lange, M.C. Santos Amaral, A critical review on membrane separation processes applied to remove pharmaceutically active compounds from water and wastewater, J. Water Process Eng., 26 (2018) 156-175.

[4] R. Rienzie, S. Ramanayaka, N.M. Adassooriya, Nanotechnology applications for the removal of environmental contaminants from pharmaceuticals and personal care products, in: M. Prasad, M. Vithanage, A. Kapley (Eds.) Pharmaceuticals and Personal Care Products: Waste Management and Treatment Technology, 2019, pp. 279-296.

[5] J. Heo, S. Kim, N. Her, C.M. Park, M. Yu, Y. Yoon, Removal of contaminants of emerging concern by FO, RO, and UF membranes in water and wastewater, in: A. Hernandez-Maldonado, L. Blaney (Eds.) Contaminants of Emerging Concern in Water and Wastewater, 2020, pp. 139-176.

[6] R. Gonzalez-Olmos, A. Penadés, G. Garcia, Electro-oxidation as efficient pretreatment to minimize the membrane fouling in water reuse processes, J. Membr. Sci., 552 (2018) 124-131.

617 [7] K. Rajwade, A.C. Barrios, S. Garcia-Segura, F. Perreault, Pore wetting in membrane
618 distillation treatment of municipal wastewater desalination brine and its mitigation by
619 foam fractionation, Chemosphere, 257 (2020) 127214.
620 [8] A. Soriano, D. Gorri, L.T. Biegler, A. Urtiaga, An optimization model for the
621 treatment of perfluorocarboxylic acids considering membrane preconcentration and
622 BDD electrooxidation, Water Res., 164 (2019) 114954.
623 [9] G. Perez, A.R. Fernandez-Alba, A.M. Urtiaga, I. Ortiz, Electro-oxidation of reverse
624 osmosis concentrates generated in tertiary water treatment, Water Res., 44 (2010) 2763-
625 2772.
626 [10] D. Rice, P. Westerhoff, F. Perreault, S. Garcia-Segura, Electrochemical self-
627 cleaning anodic surfaces for biofouling control during water treatment, Electrochem.
628 Commun., 96 (2018) 83-87.
629 [11] M. Panizza, Importance of electrode material in the electrochemical treatment of
630 wastewater containing organic pollutants, in: C. Comninellis, G. Chen (Eds.)
631 Electrochemistry for the Environment, Springer, 2010, pp. 25-54.
632 [12] Y. He, H. Lin, Z. Guo, W. Zhang, H. Li, W. Huang, Recent developments and
633 advances in boron-doped diamond electrodes for electrochemical oxidation of organic
634 pollutants, Sep. Purif. Technol., 212 (2019) 802-821.
635 [13] P.V. Nidheesh, G. Divyapriya, N. Oturan, C. Trellu, M.A. Oturan, Environmental
636 applications of boron-doped diamond electrodes: 1. Applications in water and
637 wastewater treatment, ChemElectroChem, 6 (2019) 2124-2142.
638 [14] E. Mostafa, P. Reinsberg, S. Garcia-Segura, H. Baltruschat, Chlorine species
639 evolution during electrochlorination on boron-doped diamond anodes: In-situ
640 electrogeneration of Cl_2, Cl_2O and ClO_2, Electrochim. Acta, 281 (2018) 831-840.

641 [15] A. Farhat, J. Keller, S. Tait, J. Radjenovic, Oxidative capacitance of sulfate-based
642 boron-doped diamond electrochemical system, Electrochem. Commun., 89 (2018) 14-
643 18.
644 [16] M.E.H. Bergmann, Drinking water disinfection by in-line electrolysis: Product and
645 inorganic by-product formation, in: C. Comninellis, G. Chen (Eds.) Electrochemistry
646 for the Environment, Springer, 2010, pp. 163-204.
647 [17] Y. Meas, L.A. Godinez, E. Bustos, Ozone Generation Using Boron-Doped
648 Diamond Electrodes, in: E. Brillas, C.A. Martínez-Huitle (Eds.) Synthetic Diamond
649 Films: Preparation, Electrochemistry, Characterization, and Applications, Wiley Online
650 Library, 2011, pp. 311-331.
651 [18] E. Brillas, I. Sirés, M.A. Oturan, Electro-Fenton process and related
652 electrochemical technologies based on Fenton's reaction chemistry, Chem. Rev., 109
653 (2009) 6570-6631.
654 [19] E. Brillas, A review on the photoelectro-Fenton process as efficient
655 electrochemical advanced oxidation for wastewater remediation. Treatment with UV
656 light, sunlight, and coupling with conventional and other photo-assisted advanced
657 technologies, Chemosphere, 250 (2020) 126198.
658 [20] P.V. Nidheesh, M. Zhou, M.A. Oturan, An overview on the removal of synthetic
659 dyes from water by electrochemical advanced oxidation processes, Chemosphere, 197
660 (2018) 210-227.
661 [21] G. Divyapriya, P.V. Nidheesh, Importance of Graphene in the Electro-Fenton
662 Process, ACS omega, 5 (2020) 4725-4732.
663 [22] B.S. Tawabini, K.V. Plakas, M. Fraim, E. Safi, T. Oyehan, A.J. Karabelas,
664 Assessing the efficiency of a pilot-scale GDE/BDD electrochemical system in removing
665 phenol from high salinity waters, Chemosphere, 239 (2020) 124714.

[23] L.H. Nowell, J. Hoigné, Photolysis of aqueous chlorine at sunlight and ultraviolet wavelengths—II. Hydroxyl radical production, Water Res., 26 (1992) 599-605.

[24] Z. Shu, C. Li, M. Belosevic, J.R. Bolton, M.G. El-Din, Application of a solar UV/chlorine advanced oxidation process to oil sands process-affected water remediation, Environ. Sci. Technol., 48 (2014) 9692-9701.

[25] W. Huang, M. Brigante, F. Wu, C. Mousty, K. Hanna, G. Mailhot, Assessment of the Fe(III)-EDDS complex in Fenton-like processes: from the radical formation to the degradation of bisphenol A, Environ. Sci. Technol., 47 (2013) 1952-1959.

[26] P. Soriano-Molina, J.L. García Sánchez, O.M. Alfano, L.O. Conte, S. Malato, J.A. Sánchez Pérez, Mechanistic modeling of solar photo-Fenton process with Fe3+-EDDS at neutral pH, 233 (2018) 234-242.

[27] P. Soriano-Molina, P. Plaza-Bolaños, A. Lorenzo, A. Agüera, J.L. García Sánchez, S. Malato, J.A. Sánchez Pérez, Assessment of solar raceway pond reactors for removal of contaminants of emerging concern Appl Catal B-Environ.,by photo-Fenton at circumneutral pH from very different municipal wastewater effluents, Chem. Eng. J., 366 (2019) 141-149.

[28] A.Y. Bagastyo, D.J. Batstone, I. Kristiana, W. Gernjak, C. Joll, J. Radjenovic, Electrochemical oxidation of reverse osmosis concentrate on boron-doped diamond anodes at circumneutral and acidic pH, Water Res., 46 (2012) 6104-6112.

[29] A. Soriano, D. Gorri, A. Urtiaga, Efficient treatment of perfluorohexanoic acid by nanofiltration followed by electrochemical degradation of the NF concentrate, Water Res., 112 (2017) 147-156.

[30] S. Garcia-Segura, A.B. Nienhauser, A.S. Fajardo, R. Bansal, C.L. Coonrod, J.D. Fortner, M. Marcos-Hernández, T. Rogers, D. Villagran, M.S. Wong, P. Westerhoff, Disparities between experimental and environmental conditions: Research steps toward

691 making electrochemical water treatment a reality, Curr. Opin. in Electrochem., 22
692 (2020) 9-16.
693 [31] L. Clarizia, D. Russo, I. Di Somma, R. Marotta, R. Andreozzi, Homogeneous
694 photo-Fenton processes at near neutral pH: A review, Applied Catalysis B:
695 Environmental, 209 (2017) 358-371.
696 [32] S. Miralles-Cuevas, I. Oller, J.A.S. Perez, S. Malato, Removal of pharmaceuticals
697 from MWTP effluent by nanofiltration and solar photo-Fenton using two different iron
698 complexes at neutral pH, Water Res., 64 (2014) 23-31.
699 [33] I. Salmerón, K.V. Plakas, I. Sirés, I. Oller, M.I. Maldonado, A.J. Karabelas, S.
700 Malato, Optimization of electrocatalytic H2O2 production at pilot plant scale for solar-
701 assisted water treatment, Appl Catal B-Environ., 242 (2019) 327-336.
702 [34] S. Malato, J. Blanco, A. Campos, J. Caceres, C. Guillard, J.M. Herrmann, A.R.
703 Fernandez-Alba, Effect of operating parameters on the testing of new industrial titania
704 catalysts at solar pilot plant scale, Appl. Catal. B-Environ., 42 (2003) 349-357.
705 [35] D. Schowanek, T.C.J. Feijtel, C.M. Perkins, F.A. Hartman, T.W. Federle, R.J.
706 Larson, Biodegradation of [S, S],[R, R] and mixed stereoisomers of ethylene diamine
707 disuccinic acid (EDDS), a transition metal chelator, Chemosphere, 34 (1997) 2375-
708 2391.
709 [36] E. Cuervo Lumbaque, D. Salmoria Araújo, T. Moreira Klein, E.R. Lopes Tiburtius,
710 J. Argüello, C. Sirtori, Solar photo-Fenton-like process at neutral pH: Fe(III)-EDDS
711 complex formation and optimization of experimental conditions for degradation of
712 pharmaceuticals, Catal. Today, 328 (2019) 259-266.
713 [37] M. Orama, H. Hyvönen, H. Saarinen, R. Aksela, Complexation of [S,S] and mixed
714 stereoisomers of N,N′-ethylenediaminedisuccinic acid (EDDS) with Fe(III), Cu(II),

715 Zn(II) and Mn(II) ions in aqueous solution, J. Chem. Soc., Dalton Trans., (2002) 4644-
716 4648.
717 [38] W. Huang, M. Brigante, F. Wu, K. Hanna, G. Mailhot, Development of a new
718 homogenous photo-Fenton process using Fe(III)-EDDS complexes, J. Photoch.
719 Photobio. A., 239 (2012) 17-23.
720 [39] N. Klamerth, S. Malato, A. Aguera, A. Fernandez-Alba, G. Mailhot, Treatment of
721 municipal wastewater treatment plant effluents with modified photo-Fenton as a tertiary
722 treatment for the degradation of micro pollutants and disinfection, Environ. Sci.
723 Technol., 46 (2012) 2885-2892.
724 [40] S. Miralles-Cuevas, F. Audino, I. Oller, R. Sánchez-Moreno, J.A.S. Pérez, S.
725 Malato, Pharmaceuticals removal from natural water by nanofiltration combined with
726 advanced tertiary treatments (solar photo-Fenton, photo-Fenton-like Fe (III)–EDDS
727 complex and ozonation), Sep. Purif. Technol., 122 (2014) 515-522.
728 [41] Z. Ye, E. Brillas, F. Centellas, P.L. Cabot, I. Sirés, Electro-Fenton process at mild
729 pH using Fe(III)-EDDS as soluble catalyst and carbon felt as cathode, Appl Catal B-
730 Environ., 257 (2019).
731 [42] P. Soriano-Molina, J.L. García Sánchez, S. Malato, L.A. Pérez-Estrada, J.A.
732 Sánchez Pérez, Effect of volumetric rate of photon absorption on the kinetics of
733 micropollutant removal by solar photo-Fenton with Fe3+-EDDS at neutral pH, Chem.
734 Eng. J., 331 (2018) 84-92.
735 [43] Y. Luo, W. Guo, H.H. Ngo, L.D. Nghiem, F.I. Hai, J. Zhang, S. Liang, X.C. Wang,
736 A review on the occurrence of micropollutants in the aquatic environment and their fate
737 and removal during wastewater treatment, Sci. Total Environ., 473-474 (2014) 619-641.
738 [44] N. Klamerth, N. Miranda, S. Malato, A. Agüera, A.R. Fernández-Alba, M.I.
739 Maldonado, J.M. Coronado, Degradation of emerging contaminants at low

concentrations in MWTPs effluents with mild solar photo-Fenton and TiO_2, Catal. Today, 144 (2009) 124-130.

[45] R. Xiong, Z. Lu, Q. Tang, X. Huang, H. Ruan, W. Jiang, Y. Chen, Z. Liu, J. Kang, D. Liu, UV-LED/chlorine degradation of propranolol in water: Degradation pathway and product toxicity, Chemosphere, 248 (2020).

Supplementary Information

Table SI-1. Ionic composition of simulated nanofiltration retentate and Natural water

	Natural water (mg L^{-1})	Simulated nanofiltration retentate (mg L^{-1})
HCO_3^-	813	813
Cl-	254	555
SO_4^{2-}	169	1465
Na^+	389	1050
Ca^{2+}	73	213
NH_4^+	0	18
Mg^{2+}	50	50
K^+	7.3	46
NO_3^-	11	73
$HPO4^{2-}$	0	14

774 **Table SI-2.** Characterization of urban wastewater treatment plant secondary effluent from El

775 Ejido (Almería, Spain)

	Urban wastewater treatment plant secondary effluent
Conductivity (mS cm^{-1})	2.1 - 2.3
NTU	3.1 - 5.9
pH	7.4 - 7.7
DOC	11 - 12
COD	17 - 50
HCO_3^- (mg L^{-1})	264 - 440
Cl^- (mg L^{-1})	423 - 460
SO_4^- (mg L^{-1})	127 - 140
Na^+ (mg L^{-1})	254 - 264
Ca^{2+} (mg L^{-1})	96 - 105
NH_4^+ (mg L^{-1})	22 - 35
Mg^{2+} (mg L^{-1})	66 -67
K^+ (mg L^{-1})	23 - 25
NO_3^- (mg L^{-1})	12 - 31

776 **Table SI-3.** Retention time, limit of quantification (LOQ) and maximum absorption wavelength
777 of studied microcontaminants under UPLC-UV analysis.

Microcontaminants	Retention time (min)	LOQ (μg L^{-1})	Maximum absorption (λ)
Pentaclorophenol	10.4	10	220 nm
Terbutryn	7.7	10	230 nm
Chlorphenvinfos	10.9	10	240 nm
Diclofenac	9.6	10	285 nm

778

779 **Table SI-4**. Optimal LC-QqLIT-MS/MS conditions for microcontaminant multi-residue
780 analysis.

Compound	Rt (min)	Precursor ion	Quantifier/ qualifyer	DP[a] (V)	EP[b] (V)	CE[c] (eV)	CXP[d] (V)
10,11 - Dihydrocarbamazepine	9.31	239.3	194.1	66	12	32	10
			180.2	150	10	47	11
4 -AA	5.3	204.2	56.2	45	5	30	2
			159.2	45	5	16	2
4 -AAA	6.62	246.2	228.1	46	5	18	2
			83.1	46	5	40	2
4 -DAA	5.1	232.2	113.2	48	5	17	2
			111.2	48	5	21	2
4 -FAA	6.54	232.2	214.2	60	5	18	2
			77	60	5	50	2
4 -MAA	4.75	218.2	56.1	35	5	30	2
			97.2	35	5	16	2
9-Acridinecarboxilic acid	11.63	224.2	196	63	12	36	11
			167.2	63	12	54	11
			180	63	12	42	10
Acetaminophen	5.8	152.1	110.1	40	5	20	2
			64.8	40	5	45	2
Acetamiprid	7.84	223	126	100	10	30	4
			128	50	13	25	7
Acetanilide	8	136	94	70	10	24	15
			77	70	11	40	10
Alfuzosin	7.17	390.3	235.1	50	12	40	12
			156.1	50	12	37	10
Amitriptyline	8.8	278.4	91.2	30	5	35	2
			233.1	30	5	22	2
Amoxicilin	4.91	366.1	114	70	12	30	19
			208	70	12	13	8
			349.1	70	6	18	11

Compound	Rt (min)	Precursor ion	Quantifier/ qualifyer	DP[a] (V)	EP[b] (V)	CE[c] (eV)	CXP[d] (V)
Antipyrine	7.41	189.2	77.1	48	5	51	2
			104.1	48	5	32	2
Atenolol	3.41	267.3	145.2	70	5	35	2
			190.2	70	5	27	2
Atrazine	9.93	216	174	100	13	25	10
			176	40	8	25	10
Azithromycin	7.07	749.5	83.1	50	11	110	20
			591.4	50	12	40	13
			573.3	50	8	47	14
Azoxystrobin	9.93	404.1	372.2	100	10	20	10
			329	56	10	42	6
Betamethasone	9.76	393.3	373.1	70	10	13	20
			355	70	11	18	20
			147	70	10	39	15
Buprofezin	11.69	306	201	20	11	17	5
			116	20	13	22	6
			106	20	13	40	6
C13 Caffeine	6.95	198.1	140.1	40	5	30	2
			112.2	40	5	35	2
C13 -Phenacetin	8.68	181.3	110.3	150	10	47	11
			139.3	150	10	47	11
Caffeine	6.95	195	138	20	4	27	4
			110	20	5	31	13
			123	20	5	45	5
Carbamazepine	9.38	237.2	194.3	80	5	25	2
			192.1	80	5	35	2
Carbendazim	6.15	192.3	160.1	100	10	27	4
			132.2	100	10	41	4
Cefalexin	6.43	348	158.1	60	12	13	8
			174.1	60	11	20	11
			106.1	150	10	47	11
Cefotaxime	6.76	456.1	324.1	40	5	15	3
			396.1	40	5	10	2
			241.3	40	5	20	2
Cetirizine	9.31	389.4	201	48	12	30	12
			166.2	48	12	55	8
Chlorfenvinphos	10.95	359.1	99	60	10	50	6
			155	100	8	18	10
Chlorpyriphos	12.19	352	97	55	10	55	7
			197.9	96	10	26	6
Chlortetracycline	7.37	479.2	444	100	9	31	10
			462	100	9	24	11
Ciprofloxacin	6.47	332.2	314.3	50	5	25	2
			231.2	50	5	48	2

Compound	Rt (min)	Precursor ion	Quantifier/ qualifyer	DP[a] (V)	EP[b] (V)	CE[c] (eV)	CXP[d] (V)
Citalopram	7.88	325.3	109.1	100	5	30	2
			262.1	100	5	25	2
Clarithromycin	8.87	748.4	158.4	45	5	35	2
			590.4	45	5	26	2
Clindamycin	7.88	425.2	126.1	80	11	35	7
			377.1	80	12	28	9
Clomipramine	9.05	315.2	86.1	40	5	27	2
			58.1	40	5	60	2
Clotrimazole	9.06	344.9	277.3	30	5	15	2
			165	30	5	43	2
Cotinine	3	177	80	45	5	36	2
			98	45	5	26	2
Cyclophosphamide	8.67	261.2	140	40	12	23	12
			233.2	40	8	30	8
			106	40	8	25	6
Cyprodinil	10.83	226	77	120	12	63	9
			93	120	12	80	9
D10-Carbamazepine	9.37	247.2	204.3	150	10	47	11
			202.1	150	10	47	11
Danofloxacin	6.48	358.2	340.2	100	8	31	12
			314.3	100	8	26	11
Dextromethorphan	8.1	272.4	215.1	150	10	47	11
			171.1	150	10	47	11
			173	150	10	47	11
Diatrizoic acid	5.03	632	361	80	9	35	8
			233.1	80	8	55	12
Diazepam	10.37	285.2	193.2	100	12	42	10
			154.2	100	12	36	10
Difloxacin	6.67	400.3	299	70	8	42	17
			356	70	8	30	20
Dimethoate	7.96	230	199.1	100	10	13	4
			125.1	100	10	28	4
			171	50	7	19	9
Dimethomorph	10.32	388	301	100	10	30	8
			165	100	10	45	8
			303	130	10	29	7
Diphenhydramine	8.01	256.4	167.2	40	12	21	9
			152	40	12	50	7
Diuron	10.04	233	72	60	7	50	12
			72	110	6	36	10
Domperidone	7.56	426.2	175	37	12	35	10
			147.1	37	11	55	7
Donepezil	7.51	380.4	91	65	12	63	9
			151.1	65	14	40	8

Compound	Rt (min)	Precursor ion	Quantifier/ qualifyer	DP[a] (V)	EP[b] (V)	CE[c] (eV)	CXP[d] (V)
Doxycycline	7.98	445.3	428.2	90	10	28	9
			410.2	90	10	34	10
			154.1	90	10	39	10
EDDP	7.96	278.6	234	30	11	42	14
			249.2	30	12	31	12
Enrofloxacin	6.48	360.3	245.2	80	10	37	10
			316.2	80	10	27	12
Eprosartan	8.01	425.2	135.1	79	11	47	9
			207.1	79	12	35	10
			163.2	79	10	44	5
Erithromicyn	8.45	734.6	158.3	58	5	40	2
			576.5	58	5	28	2
Famotidine	3.42	338	189.3	25	5	24	2
			259.4	25	5	15	2
Fenhexamid	10.51	302	97	80	14	30	12
			55	80	8	60	7
Fenofibrate	11.87	361.2	233.1	60	5	25	2
			139.1	60	5	35	2
Fenofibric acid	10.98	319.1	233.1	65	5	22	2
			139.1	65	5	42	2
Flecainide	7.84	415.2	301	48	12	49	7
			398.1	48	12	35	9
			98	48	12	36	15
Flumequine	9.38	262.3	244.08	50	5	21	14
			202.3	50	5	41	12
Fluoxetine	8.73	310.3	44.2	30	5	25	2
			148.2	30	5	10	2
Gabapentin	5.96	172.4	154.1	50	9	18	9
			137.2	50	9	22	7
Ifosfamide	8.49	261.1	91.9	60	5	33	2
			154.3	60	5	29	2
Imazalil	8.54	297	159	80	12	31	8
			255	80	12	25	7
Imazalil d6	8.54	302.1	159	60	10	32	4
			203	60	10	26	4
			255.1	60	10	26	4
Imidacloprid	7.45	256.1	175.1	100	10	27	4
			209.2	100	10	25	4
Iminostilbene	9.31	194	179	150	10	47	11
			167	150	10	47	11
			152	150	10	47	11
Indomethacin	10.91	358.2	139.1	50	5	25	2
			174.3	50	5	15	2
Irbesartan	9.82	429.3	207	55	12	34	5

Compound	Rt (min)	Precursor ion	Quantifier/ qualifyer	DP[a] (V)	EP[b] (V)	CE[c] (eV)	CXP[d] (V)
			195	55	12	32	14
Isoproturon	9.88	207	72	60	8	25	12
			165	60	8	20	10
Josamycin	8.77	828.6	174.2	54	12	46	13
			229.1	54	11	43	11
			600.2	54	11	37	14
Ketolorac	9.76	256.2	105.1	70	5	25	2
			178.1	70	5	34	2
Ketoprofen	10.03	255.2	105.1	47	5	33	2
			209.2	47	5	16	2
Labetalol	7.45	329.1	162.1	32	12	33	9
			90.9	32	12	67	8
			294.2	32	12	27	15
			311.2	32	12	21	7
Lansoprazole	9.29	370	252.2	45	5	15	2
			119.2	45	5	27	2
Levofloxacin	6.25	362.1	261.2	80	8	40	10
			318.2	80	8	26	15
Lidocaine	6.52	235	86	70	7	20	5
			58	70	8	50	4
Lincomycin	5.86	407.1	126.3	50	5	45	2
			359.3	50	5	23	2
Loratadine	10.7	383.1	337.3	50	5	29	2
			267.2	50	5	40	2
Mefanamic acid	11.68	242.2	224.2	36	5	34	2
			180.2	36	5	53	2
Memantine	8.1	180.3	163.1	28	12	22	10
			107.1	28	12	36	9
Mepivacaine	6.67	247.4	98.1	28	5	23	2
			70.1	28	5	53	2
Metalaxyl	9.76	280	220	85	12	20	12
			220	100	12	19	9
			192	70	12	25	9
Methadone	8.55	310.2	265.1	70	13	22	7
			105	70	11	40	20
			223	70	13	30	11
Methiocarb	10.33	226	169	44	14	13	9
			121	44	9	25	6
			107	44	9	51	5
Methotrexate	6.1	455.2	308	80	12	28	15
			175	90	12	55	15
			134	90	12	48	15
Metoclopramide	6.57	300	184	80	6	42	11
			141	80	11	66	10

Compound	Rt (min)	Precursor ion	Quantifier/ qualifyer	DP[a] (V)	EP[b] (V)	CE[c] (eV)	CXP[d] (V)
Metoprolol	6.9	268.2	116.2	30	5	25	2
			159.2	30	5	28	2
Metronidazol	5.63	172.1	128.1	35	5	20	2
			82.1	35	5	30	2
Mevastatin	11.4	391.3	185.2	55	5	25	2
			159.3	55	5	30	2
Myclobutanil	10.38	289.2	70.2	100	10	36	4
			125.1	100	10	44	4
Nadolol	6.15	310.2	254.4	45	5	30	2
			201.2	45	5	30	2
Nalidixic acid	9.25	233.2	187	45	10	35	12
			104	45	10	55	11
Naproxen	10.23	231.2	185.1	86	5	17	10
			170.1	86	5	35	10
N-desmethylcitalopram	7.85	311.3	109.1	66	12	31	7
			262.1	66	11	23	13
Nicotinamide	3.16	123.1	53.1	35	8	42	10
			80	35	12	28	8
			78	35	12	33	12
Nicotine	2.77	163.3	130	60	4	26	7
			132	60	10	20	7
			106	60	15	23	6
Nicotinic acid	3.34	124	80.1	76	6	29	13
			78.1	76	8	30	12
Nitrendipine	10.46	361	315	80	10	18	17
			329.1	80	10	15	15
			254.2	80	10	45	15
Norfloxacin	6.41	320	302.2	220	12	33	17
			233.1	220	12	33	5
O-desmethyltramadol	5.91	250.3	58.1	70	12	45	7
			232.2	70	13	17	11
O-desmethylvenlafaxine	6.76	264.1	57.9	190	9	50	6
			107	190	13	25	6
Oxcarbamazepine	8.68	253	180	73	10	44	11
			208.1	73	10	28	13
			235.9	150	10	47	11
Oxytetracycline	6.62	461.3	426.1	90	10	27	11
			443.1	90	10	19	11
Paraxanthine	6.19	181.2	124.2	50	5	25	2
			69.2	50	5	43	2
Paroxetin	8.46	330.3	192.2	70	5	25	2
			151.2	70	5	30	2
Pentoxifylline	8.02	279	181	60	10	23	10
			138	60	10	35	10

Compound	Rt (min)	Precursor ion	Quantifier/ qualifyer	DP[a] (V)	EP[b] (V)	CE[c] (eV)	CXP[d] (V)
Phenacetin	8.68	180.3	110.1	70	10	29	6
			138	70	10	22	9
			152	70	10	21	7
Pirimicarb	8.02	239	72.1	100	10	38	4
			182.1	100	10	23	4
Primidone	8.02	219.2	91.1	35	5	35	2
			162.3	35	5	16	2
Prochloraz	10.94	376.1	308	80	10	18	4
			266	80	10	23	4
Propafenone	8.47	342.4	116	69	8	32	7
			98.1	69	12	29	6
Propamocarb	4.97	189.1	101.9	29	10	25	4
			144.1	29	10	16	4
Propanolol	7.93	260	116.2	35	5	23	2
			183.2	35	5	23	2
Propyphenazone	9.43	231.3	189.2	55	5	22	2
			201.2	55	5	30	2
Pyrimethanil	10.13	200.1	107	246	12	33	6
			82.1	246	8	35	7
Quinmerac	8.37	222	204	47	10	25	12
			141	47	13	45	10
			206	46	10	24	6
Quinoxyfen	12.25	308	197	300	12	49	5
			162	300	12	61	8
Ranitidine	3.94	315.3	176.2	38	5	21	2
			130.1	38	5	30	2
Roxithromycin	8.91	837.5	158	140	8	43	15
			679.4	140	8	31	10
Salbutamol	3.42	240.3	148.2	44	5	26	2
			222.2	44	5	14	2
Sertraline	7.87	360.3	158.9	21	12	40	8
			275.1	21	12	18	6
Simazine	9.37	202.1	132	45	5	26	2
			124.2	45	5	23	2
Simvastatin	11.96	419.1	285.3	45	5	15	2
			199.1	45	5	15	2
Sotalol	3.4	273.3	255.2	45	6	14	2
			133.2	45	6	37	2
Sulfadiazine	5.68	251.2	92.1	40	5	35	2
			108.1	40	5	30	2
Sulfamethazine	6.8	279	186.2	42	5	20	2
			156.1	42	5	26	2
Sulfamethizole	6.76	271.1	156.1	80	6	20	8
			92	80	6	37	10

Compound	Rt (min)	Precursor ion	Quantifier/ qualifyer	DP[a] (V)	EP[b] (V)	CE[c] (eV)	CXP[d] (V)
			108.1	80	6	34	10
Sulfamethoxazole	7.21	254.2	156.1	47	5	21	2
			108.1	47	5	30	2
Sulfapyridine	6.06	250.1	156.1	47	5	21	2
			108.3	47	5	34	2
Sulfathiazole	5.87	256.2	156	45	5	18	2
			92.2	45	5	34	2
Sulpiride	3.66	342.3	112	47	11	34	15
			214.1	47	12	48	11
Tamoxifen	9.69	372	72	50	10	32	8
			70	50	8	75	10
			129	50	6	38	7
Tebuconazole	10.95	308	70	80	7	50	11
			125	80	10	50	6
			70	80	10	63	10
Telmisartan	9.14	515.5	497.3	40	12	47	11
			305.2	40	12	58	15
			276.2	40	12	60	7
Terbutaline	3.42	226.3	152.2	47	5	20	2
			107.1	47	5	40	2
Terbutryn	10.05	242	186	100	13	27	10
			68	100	12	60	4
Tetracycline	6.47	445.2	154.2	75	10	40	11
			410.2	75	10	27	9
Theophylline	6.45	181.1	124.2	50	8	24	19
			69.1	50	8	35	12
Thiabendazole	6.72	202	131.1	150	10	47	11
			175.1	150	10	47	11
Tramadol	6.85	264	246.1	15	8	15	3
			58	15	8	7	3
Tramadol N-oxide	7.04	280.4	135.1	70	13	32	11
			201.1	70	13	27	10
			58	70	14	47	15
			159	70	13	37	10
Trazodone	7.4	372.4	148.1	73	12	48	8
			176	73	12	35	10
Triamterene	6.66	254.6	238.1	29	12	39	12
			168.1	29	12	47	10
Trigonelline	2.65	138.2	78.2	45	8	33	12
			92.2	150	10	47	11
Trimethopim	5.95	291.3	230.2	45	5	28	2
			123.2	45	5	30	2
Vancomycin	4.75	725.3	100.3	150	10	47	11
			144.3	150	10	47	11

Compound	Rt (min)	Precursor ion	Quantifier/ qualifyer	DP[a] (V)	EP[b] (V)	CE[c] (eV)	CXP[d] (V)
Venlafaxine	7.71	278.4	58.1	50	5	45	2
			260.4	50	5	15	2
Verapamil	8.07	455.5	303.3	52	10	36	8
			260	52	12	41	14

781 [a]DP: Declustering Potential; [b]EP: Entrance Potential; [c]CE; Collision Energy; [d]CXP: Collision
782 Cell Exit Potential

783

784 **Table SI-5.** Evolution of microcontaminant removal detected in the retentate during solar-assisted AO treatment

	Concentration (ng L^{-1})										
Microcontaminants	**0 min**	**15 min**	**30 min**	**45 min**	**60 min**	**75 min**	**90 min**	**120 min**	**150 min**	**180 min**	**Removal (%)**
4AA	4579	173	101								>99
4AAA	14347		11136	8589	8346	7792	5041	4015	1287	362	98
4FAA	28357		21905	20859	18779	14167	11298	6491	2585	780	97
Carbamazepine	7068	6732		6532	6091		5159	4703	4651	3942	44
Citalopram	878		560	557	295	175	85				>99
Diatrizoic acid	1461	1382					1043	969	766	693	53
Pentoxifylline	842	726	541	564	464					442	48
Venlafaxine	2928	2127	1934	1747	1152	1042	806	195	50		>99
Gabapentin	12385		9450		7035	6741	6258	4918	3726	2727	78
Acetamiprid	471									438	7
Azoxistrobin	57	54		49			48	43	39	36	37
Imidacloprid	4525	4479	4116				3695	3227	2316	2087	54
Terbutryn	172									155	10
Azithromycin	537	414		234	182	108	56				>99
Lincomycin	705	421	0								>99
Cetirizine	1693	1624	1584		1510	1425	1312	1276	1147	1026	39
Sulpiride	4056	3805	3058	2182	1720	1173	846	396	256	13	>99
Telmisartan	1586		1562			1540		1533	1295	1274	20
N-desmethylcitalopram	479			391						350	27
Flecainide	403	341	257		209	189	162		107	96	76
Irbesartan	1554	1482		1334	1332	1313		1186	993	905	42
Iminostilbene	5775				5557	4953		4565		3406	41
Diazepam	25			25		24				22	15
Fenofibric acid	370	264	181	111	62	35					>99

Indomethacin	68	37									>99
Naproxen	928	811	775	705							>99
Propanolol	215	137									>99
Carbendazim	138		127	112	116	104	105	99	80	65	53
Dimethoate	127	118		100	77						>99
Diuron	70		67			65		59	57	47	33
Isoproturon	85	74	73	62	61	50	39	21			>99
Metalaxyl	18			17		17			15	15	16
Myclobutanil	41		41				39		39	37	11
Tebuconazole	34		33	33	33		30		28	27	20
Erithromycin	19	14	5	3							>99
Metronidazole	161	141		135	116	109	106	87			>99
Sulfathiazole	43										>99
Trimethoprim	272	185	94								>99
Levofloxacin	1929	1758		1557	918	879	451	168			>99
Alfuzosin	9	8	6	6							>99
Domperidone	34	33									>99
Propafenone	18	11									>99
Memantine	194	178	140	139	109	96	74	41			>99
Trazodone	85	51									>99

785